THE JOURNAL OF PHYSICAL CHEMISTRY Letters

LETTER

pubs.acs.org/JPCL

Formation of Secondary Organic Aerosol from the Direct Photolytic Generation of Organic Radicals

Sean H. Kessler,[†] Theodora Nah,[‡,§] Anthony J. Carrasquillo,[⊥] John T. Jayne,[#] Douglas R. Worsnop,[#] Kevin R. Wilson,[*,‡] and Jesse H. Kroll[*,†,⊥]

[†]Department of Chemical Engineering and [⊥]Department of Civil and Environmental Engineering, Massachusetts Institute of Technology, Cambridge Massachusetts 02139, United States

[‡]Chemical Sciences Division, Lawrence Berkeley National Laboratory, Berkeley California 94720, United States

[§]Department of Chemistry, University of California, Berkeley, California 94720, United States

[#]Center for Aerosol and Cloud Chemistry, Aerodyne Research Inc., Billerica, Massachusetts 01821, United States

Supporting Information

ABSTRACT: The immense complexity inherent in the formation of secondary organic aerosol (SOA)—due primarily to the large number of oxidation steps and reaction pathways involved—has limited the detailed understanding of its underlying chemistry. As a means of simplifying such complexity, here we demonstrate the formation of SOA through the photolysis of gas-phase alkyl iodides, which generates organic peroxy radicals of known structure. In contrast to standard OH-initiated oxidation experiments, photolytically initiated oxidation forms a limited number of products via a single reactive step. As is typical for SOA, the yields of aerosol generated from the photolysis of alkyl iodides depend on aerosol loading, indicating the semivolatile nature of the particulate species. However, the aerosol was observed to be higher in volatility and less oxidized than in previous multigenerational studies of alkane oxidation, suggesting that additional oxidative steps are necessary to produce oxidized semivolatile material in the atmosphere. Despite the relative simplicity of this chemical system, the SOA mass spectra are still quite complex, underscoring the wide range of products present in SOA.

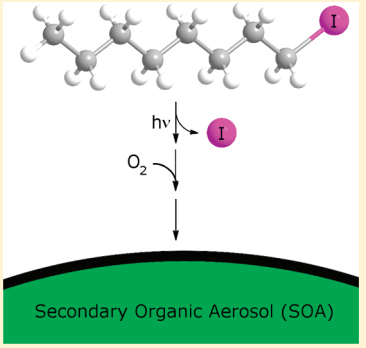

SECTION: Atmospheric, Environmental and Green Chemistry

An accurate understanding of the chemical behavior and fate of atmospheric organic species is necessary for making predictions regarding the loading and properties of organic aerosol, which together have a strong impact on both global climate and human health. Such an understanding has, however, been hindered by the immense complexity inherent in large organic reactive systems, for which the number of possible distinct species becomes nearly uncountable.[1] Most experimental studies of the products of atmospheric organic reactions, including secondary organic aerosol (SOA), involve the oxidation of a single model compound or mixture of compounds by exposure to an atmospheric oxidant over some amount of time.[2−5] Most important is oxidation by the hydroxyl radical (OH), but its high reactivity can confound laboratory studies of chemical mechanisms because multiple and sequential oxidative steps are possible during a single experiment. We present here an experimental system designed to limit oxidation processes to a single generation of products formed from a single radical precursor. In lieu of the abstraction of a hydrogen atom by OH, we use a photolabile precursor to generate SOA. Although this technique is commonly employed to study the kinetics and products of simple gas-phase reactions,[6] to our knowledge, it has not been used in the explicit study of SOA formation chemistry.

The immediate product of the reaction of a hydrocarbon with OH is typically an alkyl radical, which in turn reacts rapidly with ambient oxygen to form the peroxy radical, RO_2.[7] Peroxy radicals may subsequently react with NO or with other peroxy species to yield a distribution of products, each of which is free to react again with OH and form a new set of products. By using photolabile compounds (in this case, a series of *n*-alkyl iodides), the bimolecular hydrogen abstraction step is bypassed during the formation of the initial alkyl radical, as demonstrated in Scheme 1. In this manner, a single radical species is formed, in marked contrast to reactions that are initiated by reaction with OH. Secondary organic chemistry involving the iodine photofragment is predicted to be minimal as the C−I and H−I bonds are weak enough to make their formation energetically unfavorable.[8,9]

In the experiments presented here, gas-phase 1-octyl, 1-decyl, or 1-dodecyl iodides (98% purity, Sigma-Aldrich Co.; hereafter

Received: March 30, 2011
Accepted: May 9, 2011
Published: May 13, 2011

Scheme 1. Simplified Mechanism of Alkane Oxidation Chemistry[a]

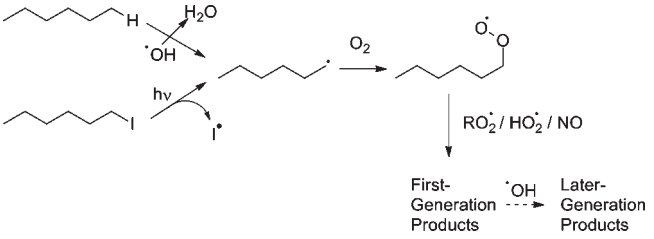

[a] In the atmosphere, and in most experimental studies, alkyl radicals are formed by abstraction of a hydrogen atom from any site on the carbon backbone by OH (top pathway); in this study, radicals are instead formed in a more controlled manner by the photolysis of alkyl iodides (bottom pathway). First-generation oxidation products will react further in the presence of OH, whereas products formed by photolysis are unreactive.

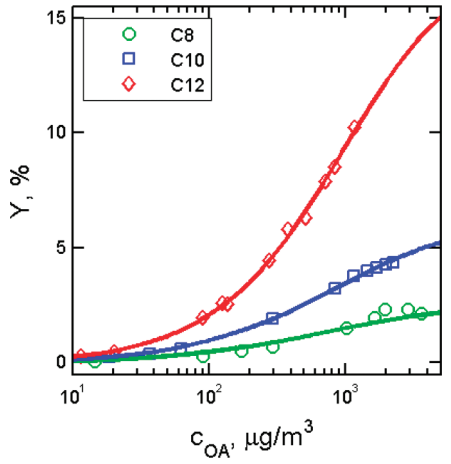

Figure 1. Adjusted organic aerosol mass yields versus total particle mass loading for the C_8, C_{10}, and C_{12} systems. Trend lines are generated using a two-parameter fit to a volatility basis set, as shown in eq 1 and Table 1.

referred to as the C_8, C_{10}, and C_{12} systems, respectively) were introduced to a flow tube reactor, with a carrier flow of synthetic air. Oxidation was initiated by irradiation by 254 nm light (which is near the absorption maximum for alkyl iodides[10]). In the absence of either light or gas-phase alkyl iodides, no particle formation was observed. However, when the precursor species was introduced to the irradiated tube, particle formation and growth was observed to occur rapidly.

As with standard chamber experiments regarding SOA generation, aerosol growth is dependent on total aerosol loading, indicating that particulate organic species are semivolatile. Following Odum et al.[11] and Donahue et al.,[12] the partitioning of the product mixture was modeled using a set of representative semivolatile products of varying volatility

$$Y = \frac{\Delta c_{OA}}{\Delta c_R} = \sum_i \alpha_i \left(1 + \frac{c_i^*}{c_{OA}}\right)^{-1} \quad (1)$$

where Y is the organic aerosol mass yield, c_{OA} is the mass concentration of particulate organics, Δc_R is the decrease in mass concentration of the gas-phase reactive species, and α_i and c_i^* are, respectively, the product yield and saturation concentration of product i.

Table 1. Product Yields by Volatility Bin and Calculated [Elemental Ratios/Oxygen and Hydrogen Content][a]

reactive species	$C_8H_{17}I$	$C_{10}H_{21}I$	$C_{12}H_{25}I$
α_1, %; ($c_1^* = 100\ \mu g\ m^{-3}$)	0.6 ± 0.5	1.0 ± 0.3	1.1 ± 0.5
α_2, %; ($c_2^* = 1000\ \mu g\ m^{-3}$)	1.9 ± 0.6	5.1 ± 0.5	16.8 ± 1.2
O/C range	0.12−0.13	0.083−0.10	0.07−0.10
H/C range	1.92−1.94	1.97−2.02	1.85−2.05
# oxygens per carbon chain	0.99−1.07	0.83−1.0	0.80−1.2

[a] Yields are determined from a two-parameter fit to eq 1, using two volatility bins with the indicated saturation concentrations. Only samples with a mass loading of at least 1 $\mu g\ m^{-3}$ were used to determine O/C and H/C ranges. The number of oxygen atoms per contiguous carbon chain is also determined from the value of O/C multiplied by the number of carbon atoms in the parent molecule. Elemental ratios given are expected to be accurate to within ±30% for O/C and ±10% for H/C.[15]

The mass yield of organic aerosol is calculated relative to the concentration of the precursor species after subtracting the mass of the iodide atom. This subtraction is performed in order to facilitate comparison of the observed aerosol yields with those reported for oxidation of *n*-alkanes.[13] This value is plotted against the total aerosol mass loading for the C_8, C_{10}, and C_{12} systems in Figure 1. As expected, the precursor species with higher molecular weights exhibit increased aerosol yields due to the lower volatility of the oxidation products. The data in each set is fitted to the volatility basis set (eq 1) using two volatility bins ($c_1^* = 100\ \mu g\ m^{-3}$ and $c_2^* = 1000\ \mu g\ m^{-3}$) for the range of c_{OA} studied.[12] Fits using a larger number of bins gave values of α that were statistically insignificant (i.e., indistinguishable from zero) or unphysical (negative). Fitted product yields (α_i) are shown in Table 1 for each of the three systems. Most of the product mass is associated with the higher-volatility bin, such that a single generation of oxidation is unlikely to produce SOA in significant yields at atmospherically relevant aerosol loadings. This is consistent with previous studies that indicate the importance of multiple oxidation generations in the formation of SOA from alkanes, especially for shorter hydrocarbon chains.[13,14] Additionally, the yields observed here are approximately one-half of those previously observed in chamber experiments of comparable alkane oxidation systems.[13] This lower yield is indicative of higher overall volatility among oxidation products; this may result from the limited number of allowed reactions, differences in RO_2 chemistry (e.g., $RO_2 + RO_2$ versus $RO_2 + NO$ reactions), or differences between the chemistry of primary alkylperoxy radicals (studied here) and secondary radicals (which are more common in OH-initiated alkane oxidation).

Chemical characterization of product aerosol mixtures was obtained from a high-resolution aerosol mass spectrometer (AMS, Aerodyne Inc.), which was operated alternately in electron impact (EI) mode (with the vaporizer set at 600 °C) or in vacuum-ultraviolet single-photon ionization (VUV-SPI) mode (with the vaporizer set at 100 °C).[5]

The high resolution of the mass spectrometer and high degree of fragmentation in the EI mode enable the estimation of elemental ratios of hydrogen to carbon atoms (H/C) and oxygen to carbon atoms (O/C), which are summarized in Table 1, using the method described by Aiken et al.[15,16] Figure 2 shows a sample EI mass spectrum for each of the C_8-, C_{10}-, and C_{12}-derived

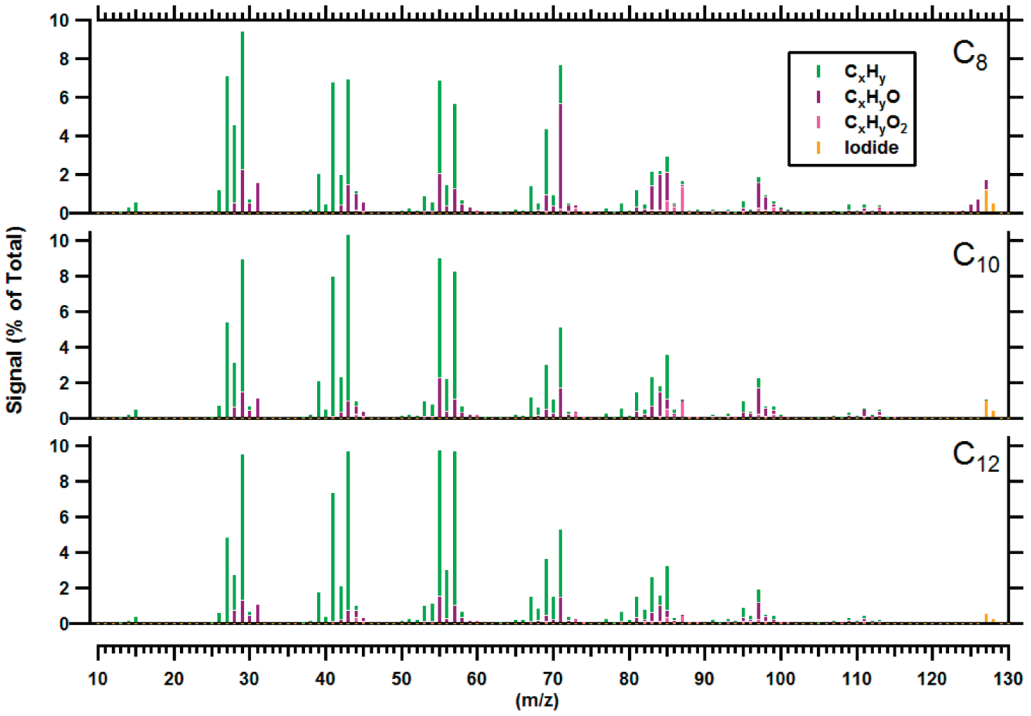

Figure 2. Sample EI mass spectra of C_8, C_{10}, and C_{12} aerosol, taken from the highest range of concentrations in each experiment and normalized by the total signal. Sticks are colored according to the oxygen content of the fragments as measured by high-resolution peak-fitting. Fragments at m/z = 127 and 128 are I^+ and HI^+, respectively. Peaks with m/z > 130 account for a minor fraction (<4%) of the total organic AMS signal.

aerosol mixtures. Mass spectra are dominated by ions of the form $C_xH_y^+$, though oxygenated fragments ($C_xH_yO_z^+$, z = 1,2) are also present. The relative presence of oxygenated fragments declines as the precursor molecular weight increases due to an increase in the number of carbon atoms. A small amount of particle-phase iodide (I^+ and HI^+) also appears in this spectrum (accounting for <2% of the total ion signal in all systems), although there are no peaks of the form $C_xH_yO_zI^+$. This suggests that the observed iodine presence comes from inorganic products (e.g., I_xO_y crystals), which have been observed in similar systems.[17] We therefore conclude that the organic aerosol formed is primarily due to the chemistry of the alkyl photofragment, with little to no influence from subsequent iodine chemistry.

The measured O/C values of the aerosol (Table 1) are lower than those measured in chamber studies of SOA from the OH-initiated oxidation of alkanes,[13] again suggesting the importance of multiple generations of oxidation in those systems. The number of oxygen atoms per contiguous carbon chain, determined by multiplying O/C by the number of carbon atoms in the precursor molecule (and assuming no reactions break or form C−C bonds), indicate that, on average, only one O atom is added per contiguous carbon chain. While such a low degree of oxidation is expected as only one oxidation step is accessed in these experiments, the identity of the low-volatility species observed must be reconciled with the apparently low number of polar functional groups. For example, even for dodecanol, one of the lowest-volatility C_{12} compounds to have only one oxygen, the expected saturation concentration is $\sim 10^4$ μg m^{-3}, at least an order of magnitude greater than what is needed to produce the mass yields observed here.[18] It therefore appears that a significant fraction of the aerosol is composed of compounds of higher molecular weight, possibly formed by oligomerization or isomerization processes. For instance, a $C_{12}OOC_{12}$ peroxide (formed by combination of two dodecyl peroxy radicals) has an expected saturation concentration of $\sim$50 μg m^{-3}, which is sufficient to contribute to SOA in the yields observed. Other potential formation mechanisms of low-volatility, slightly oxidized species are described below. It should be noted that the actual oxygen content might be somewhat greater than what is estimated here due to uncertainties in the O/C parametrization; such uncertainties may be especially large in this case because the measured product mixture is limited to a small number of individual species.[15]

AMS measurements were also carried out using VUV-SPI, a "soft" ionization technique involving a lower degree of fragmentation than that in EI and therefore improved determination of molecular species. Figure 3 shows representative VUV mass spectra from the C_8, C_{10}, and C_{12} experiments, with the dominant peaks occurring at higher values of m/z than those in the EI spectra. The spectra are reasonably complex and are dominated by ions with odd-numbered masses, indicative of molecular fragments. This is not typical of VUV spectra of organic aerosol, which tend to show molecular (even-mass) peaks.[5,19,20] This suggests that the present chemical system may contain weakly bound and/or easily photoionized species, such as organic peroxides.[21]

Major peaks in each VUV mass spectrum are clustered about m/z = 127 ($C_8H_{15}O^+$), 155 ($C_{10}H_{19}O^+$), and 183 ($C_{12}H_{23}O^+$), which correspond to the mass of the main carbon chain with one oxygen atom added (high-resolution analysis confirms these assignments as the I^+ ion contributes <1% to the total ion signal at m/z = 127). The mass differences ($\Delta(m/z)$

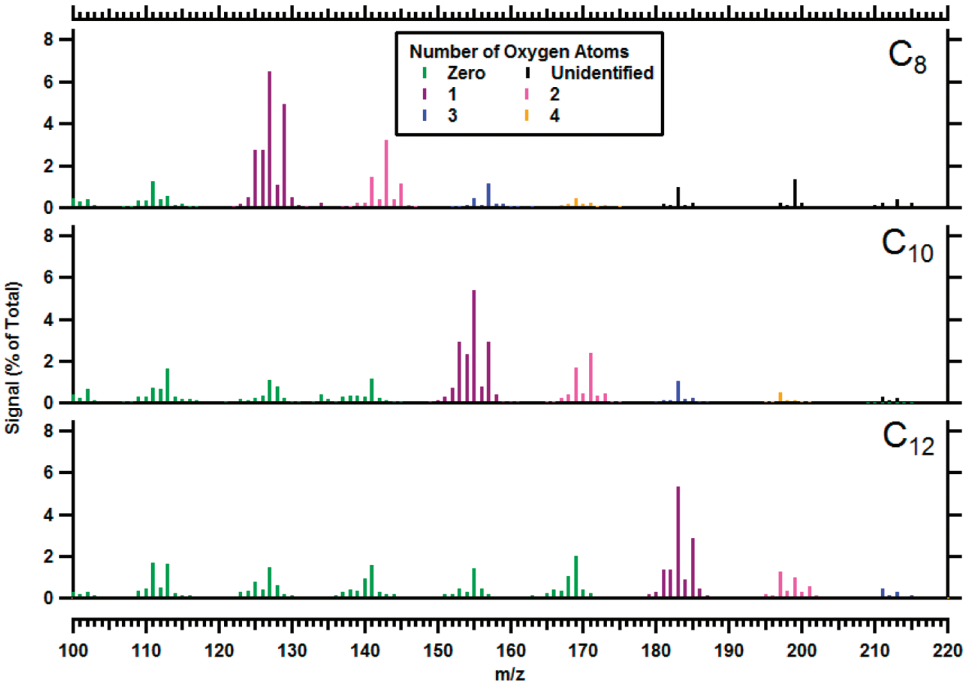

Figure 3. VUV mass spectra of the C_8, C_{10}, and C_{12} systems. The principal clusters of peaks in each case correspond to C_xO, with more highly oxidized molecules at higher masses. The number of oxygen atoms in each cluster is confirmed by high-resolution analysis. Other peaks with $m/z > 220$ are measured, though they have not been positively identified; these ions, which presumably correspond to high-molecular-weight species (such as oligomeric peroxides), account for 18−30% of the total ion signal. Peaks with $m/z < 100$, which correspond to fragment ions, account for an additional 30−42% of the total ion signal.

Scheme 2. Expected Reaction Pathways for the Alkylperoxy Radical in This Experiment[a]

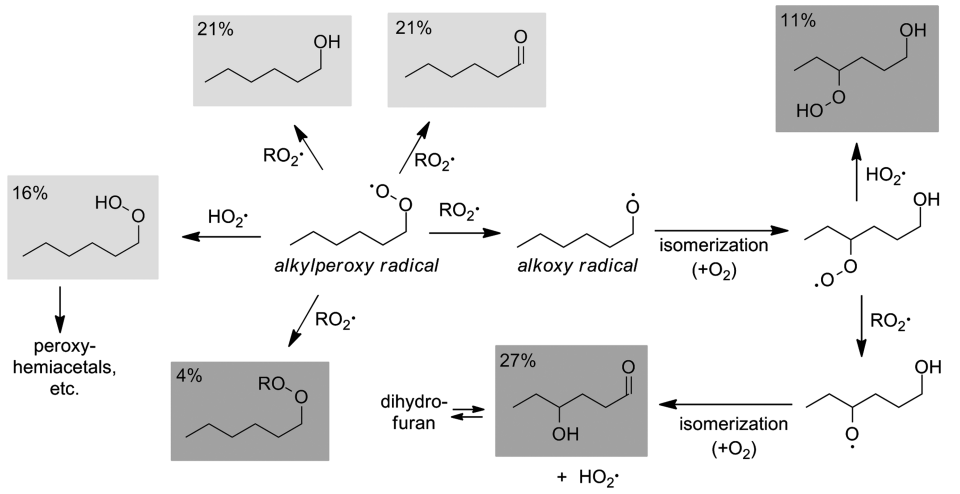

[a] Stable molecules are indicated by shaded boxes, with the more-volatile species against light gray and the less-volatile ones against dark gray. Approximate molar product yields, estimated by a kinetic model (described in the Supporting Information), are indicated in each box. The alkylperoxy radical chemistry involves not only $RO_2 + RO_2$ self-reactions, but also the reaction of RO_2 with HO_2; the latter is formed as a by-product of hydroxycarbonyl generation. Although peroxyhemiacetal and dihydrofuran products are not explicitly modeled, these products are sufficiently low in both volatility and oxygen content to agree qualitatively with the experimental results.

= 28) between these peaks are consistent with the differences between the molecular weight of the precursor species. Other significant peaks at ±2 amu may indicate various degrees of (un)saturation of the organic species being observed. The higher-mass clusters correspond to ions with multiple oxygen atoms; these minor species again suggest the presence of isomerization and chain-propagation products.

Shown in Scheme 2 are the major reactive pathways available to RO_2 radicals formed in the simple chemical system studied here (*n*-alkyl iodides + 254 nm light + air), with product yields estimated from a simple kinetic model (described in the Supporting Information). The initial radical chemistry is straightforward; the alkyl radicals (R) react with oxygen to form alkylperoxy radicals (RO_2), which mostly react with other RO_2 radicals

(reactions of alkyl and alkoxy radicals with other organic species are negligible). $RO_2 + RO_2$ reactions form volatile alcohols and carbonyls but may also produce low-volatility peroxides of the form ROOR.[22−24] Other major $RO_2 + RO_2$ products include alkoxy radicals; these can isomerize to hydroxycarbonyls, which may themselves isomerize and dehydrate to form low-volatility dihydrofuran species.[13] This pathway also generates HO_2, which will react with RO_2 radicals to form hydroperoxide species (accounting for >25% of the RO_2 reaction). ROOH species are not low enough in volatility to condense into the particle phase, but they may react with carbonyls to generate low-volatility peroxyhemiacetals.[25] The formation of these various low-volatility species—dialkyl peroxides, dihydrofurans, and peroxyhemiacetals—may explain the observation of aerosol with relatively low oxygen content. Moreover, these products may also explain the relatively complicated VUV-MS spectra shown in Figure 3 and underscore the substantial chemical complexity of SOA, even when secondary reactions and multigenerational oxidation are heavily suppressed.

Although the chemical complexity of the organic mixture may preclude the identification of individual species by the methods used here, the direct photolytic initiation of oxidation allows for the isolation of individual reaction steps, thereby simplifying the complexity associated with multiple generations of oxidation. This same general approach can also be applied to branched, cyclic, or functionalized precursors (which would most likely have to be synthesized in the laboratory) in order to study the oxidative chemistry of structurally complex species and even of later-generation products of atmospheric oxidation. Further, in the atmosphere, RO_2 will mostly react with NO and HO_2, which may lead to the formation of aerosol with very different loading and composition.[13,26] Introduction of such species will be the focus of future studies; because of the negligible role of RO_2 self-reactions in such systems, this may allow for the distribution of oxidation products to be simplified still further.

Experiments were carried out in a flow reactor, which has been described previously in detail[4,5,27] and so is described only briefly here. The reactor is made up of type-219 quartz, with a length of 130 cm and inner diameter of 2.5 cm. The effective residence time, defined by the section of the reactor exposed to 254 nm UV light from the pair of external mercury lamps, is ∼37 s. Four streams are mixed before entering the flow tube reactor, (1) 200 sccm pure O_2, (2) 30 sccm hexane (5 ppm) in N_2, (3) a variable flow rate of N_2, which is passed through a bubbler containing liquid organic iodide (98% purity, Sigma-Aldrich Co.), and (4) a makeup flow of dry N_2, such that the total flow rate in the reactor is 1 slpm. Concentrations of alkyl iodides are not measured directly but are instead estimated from known vapor pressures,[28] assuming the air from the bubbler is saturated in iodine species. Concentrations range from 240 ppb to 120 ppm. The hexane is used as a tracer for OH; concentrations did not change when the lights were turned on, indicating negligible OH-initiated secondary chemistry. Approximately 97% of the precursor is assumed to be photolyzed in the reactor, based on estimates of the photolysis rate constant from an absorption cross section of 10^{-18} cm^2 and a photon flux of 8×10^{-4} W cm^{-2}. Particle formation occurs spontaneously within the reactor, with no need for added seed nuclei.

Particles exiting the flow reactor are sampled into a scanning mobility particle sizer (SMPS, TSI, Inc.), for the measurement of mobility diameters, and a high-resolution time-of-flight aerosol mass spectrometer (Aerodyne Research, Inc.), for the measurement of both particle composition (operating in "W-mode" by EI ionization or in "V-mode" by VUV-SPI) and vacuum aerodynamic diameter (V-mode, EI). Aerosol mass loadings are obtained from combined SMPS measurements and AMS particle time-of-flight (PToF) data by multiplying the particle volume (from the SMPS) by the measured effective particle density.[27,29] No correction is made for the possible loss of gas-phase or particulate organics to the flow reactor walls.

■ ASSOCIATED CONTENT

Supporting Information. Details of the chemical kinetic model of the photochemical reactions shown in Scheme 2. This material is available free of charge via the Internet at http://pubs.acs.org.

■ ACKNOWLEDGMENT

This work was performed at the Advanced Light Source and was supported by grants from the National Science Foundation (CHE-1012809), the American Chemical Society Petroleum Research Fund (50341-DNI4), and the Director, Office of Energy Research, Office of Basic Energy Sciences, Chemical Sciences Division of the U.S. Department of Energy under Contract No. DE-AC02-05CH11231.

■ REFERENCES

(1) Kroll, J. H.; et al. Carbon Oxidation State as a Metric for Describing the Chemistry of Atmospheric Organic Aerosol. *Nat. Chem.* **2011**, *3*, 133–139.

(2) George, I. J.; Vlasenko, A.; Slowik, J. G.; Broekhuizen, K.; Abbatt, J. P. D. Heterogeneous Oxidation of Saturated Organic Aerosols by Hydroxyl Radicals: Uptake Kinetics, Condensed-phase Products, and Particle Size Change. *Atmos. Chem. Phys.* **2007**, *7*, 4187–4201.

(3) Griffin, R. J.; Cocker, D. R.; Flagan, R. C.; Seinfeld, J. H. Organic Aerosol Formation from the Oxidation of Biogenic Hydrocarbons. *J. Geophys. Res.* **1999**, *104*, 3555–3567.

(4) Kessler, S. H.; Smith, J. D.; Che, D. L.; Worsnop, D. R.; Wilson, K. R.; Kroll, J. H. Chemical Sinks of Organic Aerosol: Kinetics and Products of the Heterogeneous Oxidation of Erythritol and Levoglucosan. *Environ. Sci. Technol.* **2010**, *44*, 7005–10.

(5) Smith, J. D.; Kroll, J. H.; Cappa, C. D.; Che, D. L.; Liu, C. L.; Ahmed, M.; Leone, S. R.; Worsnop, D. R.; Wilson, K. R. The Heterogeneous Reaction of Hydroxyl Radicals with Sub-micron Squalane Particles: A Model System for Understanding the Oxidative Aging of Ambient Aerosols. *Atmos. Chem. Phys. Discuss.* **2009**, *9*, 3945–3981.

(6) Basco, N.; James, D. G. L.; Suart, R. D. A Quantitative Study of Alkyl Radical Reactions by Kinetic Spectroscopy. Part I. Mutual Combination of Methyl Radicals and Combination of Methyl Radicals with Nitric Oxide. *Int. J. Chem Kinet.* **1970**, *2*, 215–234.

(7) Atkinson, R. Atmospheric Chemistry of VOCs and NO_x. *Atmos. Environ.* **2000**, *34*, 2063–2101.

(8) Kroll, J. H.; Seinfeld, J. H. Chemistry of Secondary Organic Aerosol: Formation and Evolution of Low-Volatility Organics in the Atmosphere. *Atmos. Environ.* **2008**, *42*, 3593–3624.

(9) Benson, S. W. *Thermochemical Kinetics*; Wiley: New York, 1968; Vol. 223.

(10) Roehl, C. M.; Burkholder, J. B.; Moortgat, G. K.; Ravishankara, A. R.; Crutzen, P. J. Temperature Dependence of UV Absorption Cross Sections and Atmospheric Implications of Several Alkyl Iodides. *J. Geophys. Res.* **1997**, *102*, 12819–12829.

(11) Odum, J. R.; Hoffmann, T.; Bowman, F.; Collins, D.; Flagan, R. C.; Seinfeld, J. H. Gas/Particle Partitioning and Secondary Organic Aerosol Yields. *Environ. Sci. Technol.* **1996**, *30*, 2580–2585.

(12) Donahue, N. M.; Robinson, A. L.; Stanier, C. O.; Pandis, S. N. Coupled Partitioning, Dilution, and Chemical Aging of Semivolatile Organics. *Environ. Sci. Technol.* **2006**, *40*, 2635–2643.

(13) Lim, Y. B.; Ziemann, P. J. Products and Mechanism of Secondary Organic Aerosol Formation from Reactions of *n*-Alkanes with OH Radicals in the Presence of NO_x. *Environ. Sci. Technol.* **2005**, *39*, 9229–9236.

(14) Robinson, A. L.; Donahue, N. M.; Shrivastava, M. K.; Weitkamp, E. A.; Sage, A. M.; Grieshop, A. P.; Lane, T. E.; Pierce, J. R.; Pandis, S. N. Rethinking Organic Aerosols: Semivolatile Emissions and Photochemical Aging. *Science* **2007**, *315*, 1259–62.

(15) Aiken, A. C.; DeCarlo, P. F.; Jimenez, J. L. Elemental Analysis of Organic Species with Electron Ionization High-Resolution Mass Spectrometry. *Anal. Chem.* **2007**, *79*, 8350–8358.

(16) Aiken, A. C.; et al. O/C and OM/OC Ratios of Primary, Secondary, and Ambient Organic Aerosols with High-Resolution Time-of-Flight Aerosol Mass Spectrometry. *Environ. Sci. Technol.* **2008**, *42*, 4478–4485.

(17) Jimenez, J. L.; Bahreini, R.; Cocker, D. R., III; Zhuang, H.; Varutbangkul, V.; Flagan, R. C.; Seinfeld, J. H.; O'Dowd, C. D.; Hoffmann, T. New Particle Formation from Photooxidation of Diiodomethane (CH_2I_2). *J. Geophys. Res.* **2003**, *108*, 4318.

(18) Rose, A.; Papahronis, B.; Williams, E. Experimental Measurement of Vapor−Liquid Equilibria for Octanol−Decanol and Decanol−Dodecanol Binaries. *Ind. Eng. Chem. Chem. Eng. Data Ser.* **1958**, *3*, 216–219.

(19) Gloaguen, E.; Mysak, E. R.; Leone, S. R.; Ahmed, M.; Wilson, K. R. Investigating the Chemical Composition of Mixed Organic−Inorganic Particles by "Soft" Vacuum Ultraviolet Photoionization: The Reaction of Ozone with Anthracene on Sodium Chloride Particles. *Int. J. Mass Spectrom.* **2006**, *258*, 74–85.

(20) Mysak, E. R.; Wilson, K. R.; Jimenez-Cruz, M.; Ahmed, M.; Baer, T. Synchrotron Radiation Based Aerosol Time-of-Flight Mass Spectrometry for Organic Constituents. *Anal. Chem.* **2005**, *77*, 5953 5960.

(21) Shuman, N. S.; Bodi, A.; Baer, T. Heats of Formation of *t*-Butyl Peroxy Radical and *t*-Butyl Diazyl Ion: RRKM vs SSACM Rate Theories in Systems with Kinetic and Competitive Shifts. *J. Phys. Chem. A* **2010**, *114*, 232–240.

(22) Ziemann, P. J. Evidence for Low-volatility Diacyl Peroxides as a Nucleating Agent and Major Component of Aerosol Formed from Reactions of O_3 with Cyclohexene and Homologous Compounds. *J. Phys. Chem. A* **2002**, *106*, 4390–4402.

(23) Ng, N. L.; et al. Secondary Organic Aerosol (SOA) Formation from Reaction of Isoprene with Nitrate Radicals (NO_3). *Atmos. Chem. Phys.* **2008**, *8*, 3163–3226.

(24) Noell, A. C.; Alconcel, L. S.; Robichaud, D. J.; Okumura, M.; Sander, S. P. Near-Infrared Kinetic Spectroscopy of the HO_2 and $C_2H_5O_2$ Self-Reactions and Cross Reactions. *J. Phys. Chem. A* **2010**, *114*, 6983–6995.

(25) Tobias, H. J.; Ziemann, P. J. Kinetics of the Gas-Phase Reactions of Alcohols, Aldehydes, Carboxylic Acids, and Water with the C13 Stabilized Criegee Intermediate Formed from Ozonolysis of 1-Tetradecene. *J. Phys. Chem. A* **2001**, *105*, 6129–6135.

(26) Kroll, J. H.; Ng, N. L.; Murphy, S. M.; Flagan, R. C.; Seinfeld, J. H. Secondary Organic Aerosol Formation from Isoprene Photooxidation. *Environ. Sci. Technol.* **2006**, *40*, 1869–1877.

(27) Kroll, J. H.; Smith, J. D.; Che, D. L.; Kessler, S. H.; Worsnop, D. R.; Wilson, K. R. Measurement of Fragmentation and Functionalization Pathways in the Heterogeneous Oxidation of Oxidized Organic Aerosol. *Phys. Chem. Chem. Phys.* **2009**, *11*, 8005–8014.

(28) Li, J. C. M.; Rossini, F. D. Vapor Pressures and Boiling Points of the l-Fluoroalkanes, l-Chloroalkanes, l-Bromoalkanes, and l-Iodoalkanes, C1 to C20. *J. Chem. Eng. Data* **1961**, *6*, 268–270.

(29) DeCarlo, P.; Slowik, J. G.; Worsnop, D. R.; Davidovits, P.; Jimenez, J. L. Particle Morphology and Density Characterization by Combined Mobility and Aerodynamic Diameter Measurements. Part 1: Theory. *Aerosol Sci. Technol.* **2004**, *38*, 1185–1205.